Springer

KSME

Journal of Mechanical Science and Technology 30 (11) (2016) 4909~4917
www.springerlink.com/content/1738-494x(Print)/1976-3824(Online)
DOI 10.1007/s12206-016-1010-z

A hybrid method of modified NSGA-II and TOPSIS for lightweight design of parameterized passenger car sub-frame †

Dengfeng Wang[1], Rongchao Jiang[2,*] and Yinchong Wu[1]

[1]*State Key Laboratory of Automotive Simulation and Control, Jilin University, Changchun 130022, China*
[2]*College of Mechanical and Electronic Engineering, Qingdao University, Qingdao 266071, China*

(Manuscript Received September 7, 2015; Revised June 10, 2016; Accepted June 14, 2016)

Abstract

This paper presents a hybrid method integrating modified NSGA-II and TOPSIS, used for lightweight design of the front sub-frame of a passenger car. Firstly, the FE model of the sub-frame is constructed and is validated by modal test. Then, the strength performance of the sub-frame is analyzed under four typical load conditions consisting of braking, acceleration, steady state cornering and vertical bump. After that, a parameterized model of the sub-frame, in which 12 geometric parameters are defined as design variables, is developed based on the mesh morphing technology. Subsequently, modified NSGA-II is employed for multi-objective optimization of the sub-frame considering weight, maximum von-Mises stress and first order natural frequency as three conflicting objective functions. Accordingly, a set of Pareto-optimal solutions are obtained from the optimization process. Finally, the entropy weight theory and TOPSIS method are adopted to rank all these solutions from the best to the worst for determining the best compromise solution. In addition, the effectiveness of the proposed hybrid lightweight design method is demonstrated by the comparisons among baseline design and optimum solutions.

Keywords: Sub-frame; Lightweight design; Mesh morphing technology; Multi-objective optimization; TOPSIS

1. Introduction

Lightweight design of vehicle components has attracted much attention by automotive manufacturers in recent years, due to the need for reducing fuel consumption and greenhouse gas emission, as well as the increasing desire for better vehicle performance [1]. Particularly, the lightweight design of front sub-frame, which is designed to carry engine and other suspension components on front wheel drive passenger cars, is critical to the improvement of vehicle performance such as ride comfort, handling stability and NVH (Noise, vibration and harshness) performance.

Generally, the lightweight design can be addressed from three aspects of applications of novel materials, advanced processing technology and structural optimization. In the structural optimization of automotive components, most of the reported work is concentrated only on the size optimization which achieves mass reduction mainly by optimizing the thickness of different panels [2-5]. However, due to the fairly complex geometrical shape of the sub-frame, shape optimization has greater potential in weight saving compared with traditional size optimization. Although the shape optimization has many positive characteristics, it is difficult in defining complex shape design variables during the optimization process. Consequently, the mesh morphing technology is employed in this research to address the challenge of shape change of the Finite element (FE) model. The mesh morphing technique is originated from the computer graphics and it has been introduced to the optimization design of vehicle components by many researchers. Padmanaban et al. [6] presented a multi-disciplinary optimization study on the sport utility vehicle to minimize the BIW (Body in white) mass while meeting crash and NVH constraints. The mesh morphing technology was used to parameterize the FE models. Wang et al. [7] applied the mesh morphing technology to the retrofit design of a baseline car model for shortening the lead time of car model development and reducing development cost. Fang et al. [8] proposed a meta-model-based multi-objective shape optimization methodology for the lightweight design of BIW, where the mesh morphing technology was employed to define the shape variables.

The lightweight design of sub-frame is driven by many competing criteria such as weight, stiffness, strength and natural frequency. It should be pointed out that all these objectives should be met simultaneously, which inherently follows a multi-objective optimization process. The evolutionary algorithms are usually used to cope with the multi-objective prob-

*Corresponding author. Tel.: +86 532 85953716, Fax.: +86 532 85953716
E-mail address: jrch123@126.com
† Recommended by Associate Editor Rongchao Jiang

lem. A set of compromised solutions called Pareto set can be obtained as the optimal result of this problem [9]. One of the most popular evolutionary algorithms is elitist Non-dominated sorting genetic algorithm (NSGA-II), which is first proposed by Deb [10] and has been widely applied in the lightweight design of vehicle components. Cui et al. [11] proposed a new method for lightweight design of an automotive door assembly with discrete and continuous variables. The discrete variables were the material types, and continuous variables were the thicknesses of the panels. The design problem was formulated as a multi-objective non-linear mathematical programming problem which was solved using NSGA-II algorithm. Su et al. [12] employed the NSGA-II to solve the multi-objective optimization problem of the bus body. The objective was to minimize the weight and maximize the torsional stiffness of the bus body under the constraints of strength and rollover safety. Hu et al. [13] developed the lightweight design of the BIW from the point of view of NVH and strength performance, and the response surface method was applied to formulate the objective of optimization solved by the NSGA-II algorithm. However, density scale which is used in NSGA-II for distribution of design vectors and preventing population accumulation has deficiencies in solving multi-objective problems with more than two objective functions [14]. Therefore, a new diversity preserving algorithm called ε-elimination algorithm is employed in this paper to enhance the performance of NSGA-II in terms of diversity of population and Pareto fronts. It makes the modified NSGA-II much more stability for the optimization problems with any number of objective functions.

Once the global Pareto-optimal solutions are obtained, it is desired to choose one of the solutions for implementation. Hence, the Shannon entropy weight theory and Technique for ordering preferences by similarity to ideal solution (TOPSIS) method are adopted to rank these Pareto solutions from best to worst for determining the best compromise solution. It simultaneously has the minimum distance from an ideal point and maximum distance from a nadir point.

In this study, mesh morphing technology and modified NSGA-II algorithm are simultaneously employed to perform the multi-objective optimization for the lightweight design of the front sub-frame. The weight, maximum von-Mises stress and first order natural frequency of the sub-frame are considered as conflicting objective functions, while twelve geometrical parameters are taken as design variables. The sub-frame's stiffness and intervals between neighbor order frequencies are taken into consideration as well. Then, a set of Pareto solutions are obtained by solving the multi-objective optimization problem using modified NSGA-II algorithm, which uses ε-elimination diversity algorithm instead of crowding distance to enhance the diversity preserving performance. Moreover, the best compromise solution is determined from the Pareto solutions based on entropy weight and TOPSIS method. Finally, the final optimal design is compared with the original design to illustrate the capability of the proposed hybrid method in lightweight design of vehicle components.

2. Methods

2.1 Mesh morphing technology

Mesh morphing technology, which is originated from the computer graphics, has been successfully applied to achieve fast modification of parameterized FE models in engineering optimization problems [15]. The morphing of FE models is accomplished through transforming one source mesh into another target mesh only by moving locations of nodes without creating or removing nodes and elements. In this process, the connections between these nodes or elements remain unchanged, and the material properties and boundary conditions remain unchanged as well.

The concepts of fixed nodes, control nodes and deformable nodes are used in the mesh morphing techniques for FE models. Namely, fixed nodes determine the boundary of the deformable zone of the mesh. The control nodes are defined to drive the morphing, and a displacement vector with a one-to-one mapping between the source and target node will be applied to these control nodes during the transformation. The displacement vector $\boldsymbol{D}_i$ can be expressed as:

$$\mathbf{D}_i = \mathbf{TM} \cdot \mathbf{CN}_i - \mathbf{CN}_i \tag{1}$$

$$\mathbf{TM} = \begin{bmatrix} \cos\alpha\cos\beta & \cos\alpha\sin\beta\sin\gamma - \sin\alpha\cos\gamma & \cos\alpha\sin\beta\cos\gamma + \sin\alpha\sin\gamma \\ \sin\alpha\cos\beta & \sin\alpha\sin\beta\sin\gamma + \cos\alpha\cos\gamma & \sin\alpha\sin\beta\cos\gamma - \cos\alpha\sin\gamma \\ -\sin\beta & \cos\beta\sin\gamma & \cos\beta\cos\gamma \end{bmatrix} \tag{2}$$

where $\boldsymbol{CN}_i$ is the vector of control node coordinate and $\boldsymbol{TM}$ is the transformation matrix. In the transformation matrix, α, β and γ are rotations around local Z-axis, Y-axis and X-axis, respectively.

Moreover, deformable nodes correspond to the nodes that will be morphed in order to follow the transformation applied to the control nodes. The new positions of deformable nodes can be calculated by:

$$\mathbf{DN}_i^{new} = f(\mathbf{D}_i, \varphi, \phi) \cdot \mathbf{DN}_i^{current} \tag{3}$$

where $\mathbf{DN}_i^{current}$ and $\mathbf{DN}_i^{new}$ represent the current and new position of deformable node i, respectively. The $f(\mathbf{D}_i, \varphi, \phi)$ is a morphing shape function, in which the values of φ and ϕ are used to define the first derivative of shape function for modifying the curvature of the deformable region.

There are various commercial tools for mesh morphing of FE models in a user-friendly and application-oriented way. The most efficient one is Meshworks/Morpher. The most commonly used mesh morphing techniques within Meshworks/Morpher are free form morphing and control block morphing. They are different in the type of morphing shape function. The free form morphing uses the direct morphing approach, and the shape function is described by a set of parabolic or spherical polynomial equations. On the other hand, the indirect morphing approach is employed in the control

block morphing, where the shape function is a linear polynomial equation.

2.2 Modified NSGA-II

The NSGA-II is one of the most efficient and popular multi-objective evolutionary algorithm, which is first proposed by Deb [10]. In addition to standard GA operators including selection, crossover and mutation, a fast non-dominated sorting approach, an elitist strategy and an efficient crowding distance estimation procedure have been introduced into the NSGA-II. It should be noted that maintaining a diverse population is an important consideration in multi-objective evolutionary algorithm. Therefore, the NSGA-II adopts crowding distance measure, instead of fitness sharing parameter used by NSGA, to obtain a uniform spread of solutions along the Pareto front. The crowding distance provides an estimate of the density of solutions surrounding a particular solution in the population. Thus, to promote diversity, a solution having higher value of crowding distance is preferred over the solution with a lower crowding distance in removal process.

To calculate the crowding distance for a set of population members, the set is first sorted according to each objective function in ascending order of that objective value. Thereafter, for each objective function, the boundary individual is assigned an infinite crowding distance so that the boundary individuals can be copied to next population unconditionally. For all other intermediate individuals, the crowding distance (CD_i^k) can be calculated as follows:

$$CD_i^k = \frac{f_{i+1}^k - f_{i-1}^k}{f_{\max}^k - f_{\min}^k} \tag{4}$$

where f_{i-1}^k and f_{i+1}^k denote the kth objective function of the (i-1)th and (i+1)th individual, respectively. $f_{\min}^k$ and $f_{\max}^k$ represent the minimum and maximum of the kth objective function, respectively.

The overall Crowding distance (CD_i) is calculated as the sum of the individual crowding distances with respect to each objective, which can be defined as:

$$CD_i = \sum_{k=1}^{r} CD_i^k \tag{5}$$

where r is the number of objective functions.

It should be noted that, for the bi-objective optimization problems, ascending sorting of the solutions of a Pareto front according to one objective will consequently lead to descending sorting of these solutions corresponding to the other objective. In other words, the solution's neighbors on either side remain unchanged in the sorting procedure for two-objective optimization problems. However, this is not the case for optimization problems with more than two objective functions. The nearest neighbors of solution may be different in each dimension of the objective space. The overall crowding distance of a solution calculated in this way may not exactly reflect the true measure of diversity for the multi-objective optimization problems with more than two objectives.

To enhance the diversity preserving performance of NSGA-II, the ε-elimination diversity algorithm is adopted to replace the crowding distance. It makes the modified NSGA-II much more stable for the optimization problems with any number of objective functions [14].

The main steps of modified NSGA-II which uses both non-dominated sorting procedure and ε-elimination diversity preserving approach are described as follows:

Step 1: Randomly initiate a parent population of size N based on the problem range and constraints.

Step 2: Perform non-dominated sorting of parent population and classify them into several fronts.

Step 3: Generate offspring population from the parent population using GA operators of selection, crossover and mutation.

Step 4: Combine the parent and offspring population to create a combined population with size of 2N.

Step 5: Remove the ε-similar individuals from the combined population based on a value of ε as the elimination threshold. At the same time, randomly generate individuals to re-fill the population to size of 2N.

Step 6: Perform non-dominated sorting of the combined population to assign different fronts according to increasing order of dominance.

Step 7: Constitute the next parent population using the best fronts from the top of the sorted list until the population size exceeds N. Remove an exact number of ε-similar individuals from the last allowed front to match the size of the next parent population through adjusting the value of threshold ε.

Step 8: Repeat the procedure from step 3 after creating the new parent population if the termination criterion is not satisfied. Otherwise, stop and output the non-dominated solution set.

2.3 TOPSIS method

TOPSIS method, which was originally proposed by Hwang and Yoon, is of great use for solving multiple criteria decision making problems by ranking the possible alternatives through measuring Euclidean distances [16-19]. Its fundamental concept is that the selected alternative should simultaneously have the shortest distance from the Positive ideal solution (PIS) and the longest distance from the Negative ideal solution (NIS).

The non-dominated solutions obtained from modified NSGA-II can be taken as the decision making matrix, which is defined as:

$$\mathbf{X} = \begin{bmatrix} x_{11} & x_{12} & \cdots & x_{1n} \\ x_{21} & x_{22} & \cdots & x_{2n} \\ \cdots & \cdots & \cdots & \cdots \\ x_{m1} & x_{m2} & \cdots & x_{mn} \end{bmatrix} \tag{6}$$

where $x_{ij}, i = 1,2,\cdots,m;\ j = 1,2,\cdots,n$ represents the result of

the *j*th objective function for the *i*th Pareto solution; *m* is the number of Pareto solutions and *n* is the number of objective functions.

According to TOPSIS technique, the defined decision making matrix can be normalized to the non-scaled matrix using the following formula:

$$r_{ij} = \frac{x_{ij}}{\sqrt{\sum_{i=1}^{m} x_{ij}^2}} \tag{7}$$

where r_{ij} denotes the normalized value of x_{ij}.

Generally, the relative importance of each objective may be different. The corresponding weights of the objectives can be calculated using entropy method. It is a measure of uncertainty in the information formulated using probability theory. The entropy values e_j can be determined as:

$$e_j = -k\sum_{i=1}^{m} p_{ij} \ln p_{ij} \tag{8}$$

where k is the entropy constant and is equal to $1/\ln(m)$; p_{ij} is the projection value of r_{ij}, $p_{ij} = r_{ij} \Big/ \sum_{i=1}^{m} r_{ij}$.

The weight for each objective function can be obtained:

$$w_j = \frac{d_j}{\sum_{j=1}^{n} d_j} \tag{9}$$

where $d_j = 1\text{-}e_j$ is the deviation degree of the *j*th optimization objective. Generally speaking, a higher deviation degree indicates that it provides more information and thus this objective will have higher weight.

The weighted normalized value v_{ij} is then calculated as:

$$v_{ij} = w_j r_{ij} \qquad \sum_{j=1}^{n} w_j = 1 \tag{10}$$

where w_j is the weight of the *j*th objective.

Now, the Positive ideal solution (PIS) and Negative ideal solution (NIS) are determined for calculating the distance of an alternative from the best and worst alternatives. The PIS and NIS are determined as follows:

$$\begin{cases} A^+ = \{v_1^+, v_2^+, \cdots, v_n^+\} \\ A^- = \{v_1^-, v_2^-, \cdots, v_n^-\} \end{cases} \tag{11}$$

where A^+ denotes the PIS and A^- denotes the NIS.

If the objective function is to be maximized, which means the characteristic is larger-the-better, the PIS and NIS are respectively determined by:

$$\begin{cases} v_j^+ = \max_i \{v_{ij}, j = 1, 2, \cdots, n\} \\ v_j^- = \min_i \{v_{ij}, j = 1, 2, \cdots, n\} . \end{cases} \tag{12}$$

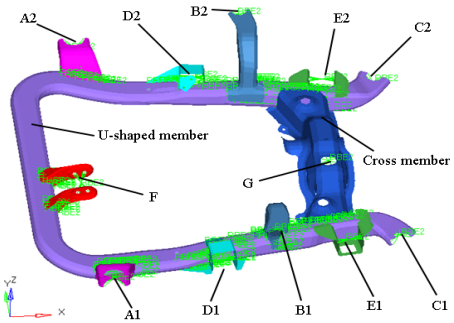

Fig. 1. FE model of the sub-frame.

If the objective function is to be minimized, which means the characteristic is smaller-the-better, the PIS and NIS are respectively determined by:

$$\begin{cases} v_j^+ = \min_i \{v_{ij}, j = 1, 2, \cdots, n\} \\ v_j^- = \max_i \{v_{ij}, j = 1, 2, \cdots, n\} . \end{cases} \tag{13}$$

The separation of each alternative from PIS and NIS can be determined by the Euclidean distance, which is defined in the following equations:

$$\begin{cases} S_i^+ = \sqrt{\sum_{j=1}^{n} (v_{ij} - v_j^+)^2} \\ S_i^- = \sqrt{\sum_{j=1}^{n} (v_{ij} - v_j^-)^2} \end{cases} \tag{14}$$

where S_i^+ represents the distance between the *i*th alternative and PIS, and S_i^- denotes the distance between the *i*th alternative and NIS.

Finally, the relative closeness of a particular alternative to the ideal solution is expressed as:

$$C_i = \frac{S_i^-}{S_i^+ + S_i^-} . \tag{15}$$

The closeness will be ranked in descending order and the Pareto solution with the maximum value of C_i will be the best choice.

3. Finite element analysis

3.1 Finite element modeling

The front sub-frame considered in this paper consists of a U-shaped member made of steel tube using the hydroforming technology, a cross member and nine mounting brackets. The cross member and brackets are welded on the U-shaped member, as shown in Fig. 1. At points A1, A2, B1, B2, C1 and C2, the sub-frame is fastened together with the BIW using mounting bushings. The left and right lower control arms of suspension system are attached to the sub-frame by means of bolted joints at points D1, D2, E1 and E2, respectively. Points F and

Table 1. Comparison between analytical and experimental frequencies.

Mode number	Natural frequencies (Hz)		Relative error (%)	Mode shape
	Analytical	Experimental		
1~6	0	0		Rigid mode
7	86.70	89.03	-2.69	1st torsion
8	143.01	137.20	4.06	1st bending
9	163.77	155.09	5.30	
10	224.45	217.86	2.94	
11	234.85	239.18	-1.85	
12	274.81	289.86	-5.48	

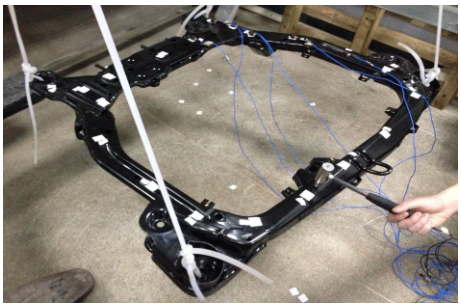

Fig. 2. Modal test of the sub-frame.

G are used to support the engine with rubber bushings. The FE model of the sub-frame (Fig. 1) containing 68051 elements was developed using shell elements, for giving a good relationship between stress results and simulation time consumption.

3.2 Modal analysis

As it is well known, a main function of the sub-frame is to isolate the undesirable excitations caused by road roughness and engine vibrations. In order to achieve low structural transmissibility, it is important to ensure that the excited frequency does not match the natural frequency of sub-frame to avoid resonance. Therefore, it is essential to analyse the frequency response related to the sub-frame. In this paper, the natural frequencies of the sub-frame were calculated with freedom boundary constraint. Simultaneously, the modal test of the sub-frame was performed in a free hanging state using impact hammer testing method, as shown in Fig. 2. The natural frequencies obtained from FE analysis and modal testing were illustrated in Table 1. It can be seen from this table that the analytical natural frequencies were in good agreement with the experimental frequencies. In addition, a comparison between the analytical and experimental mode shape for the first torsion mode was conducted to confirm the validity for the FE model of the sub-frame, as shown in Fig. 3.

3.3 Strength analysis

The front sub-frame should possess sufficient strength and stiffness to support the suspension, engine and steering gear

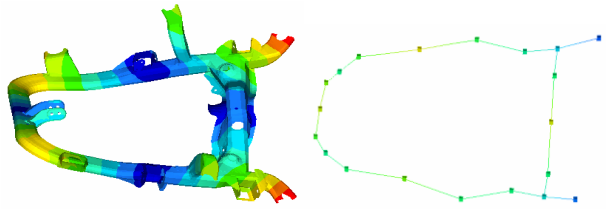

(a) Analytical (b) Experimental

Fig. 3. First torsion mode shape of the sub-frame.

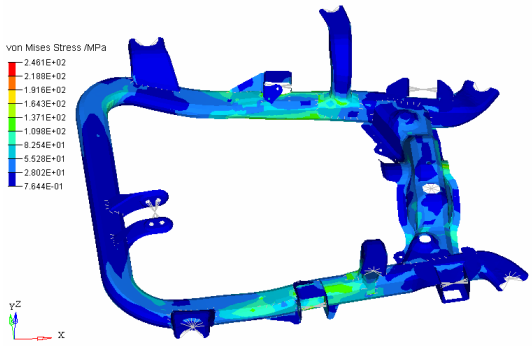

(a) Stress distribution

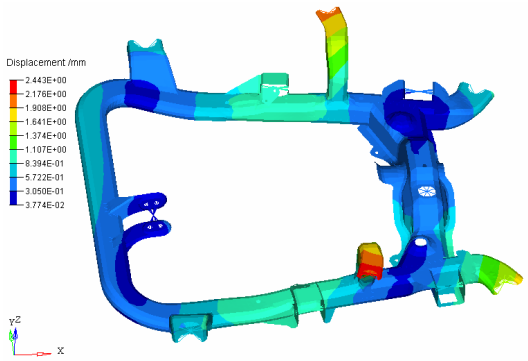

(b) Displacement contour

Fig. 4. Static analysis results of the sub-frame for acceleration load case.

box under severe operating conditions. In addition, the sub-frame also contributes to durability and collision performance. Thus, four main in-service load cases consisting of braking, acceleration, steady state cornering and vertical bump, were adopted for static analysis of the sub-frame in this study. The forces imposed on the sub-frame at connect joints for the four typical load cases were obtained by multi-body dynamic analysis. Then, the linear stress analyses of the sub-frame were performed using MSC.Nastran with inertia relief algorithm to obtain stresses for each load case.

Fig. 4 shows the stress distribution and displacement contour of the sub-frame under the acceleration load case. As it can be clearly seen in this figure, the stress concentration area is located around the front mounting bracket for connecting lower control arm. However, the stress level of the sub-frame is not high. The maximum von Mises stress is not more than 246.1 MPa. This indicated that the sub-frame has great resid-

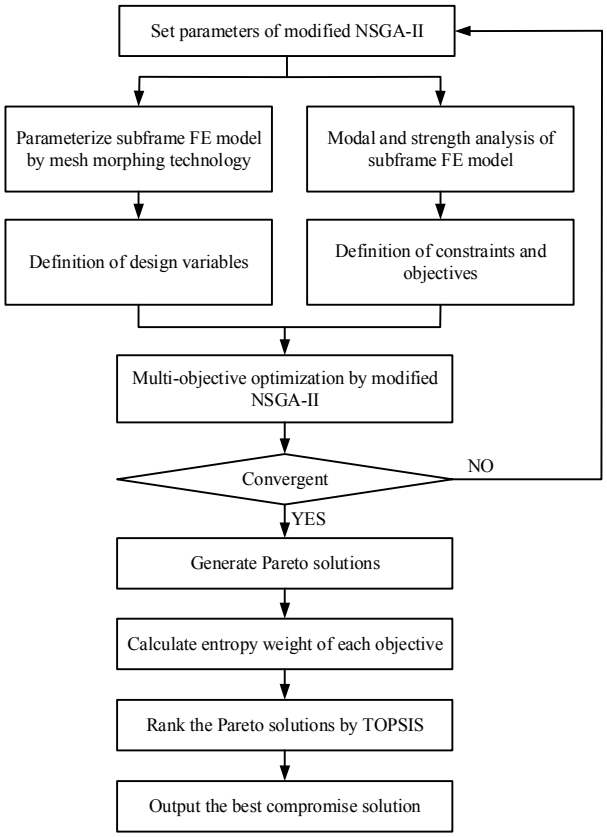

Fig. 5. Flowchart of multi-objective optimization procedure.

ual strength and potential for further lightweight design.

4. Multi-objective optimization for lightweight design of sub-frame

4.1 Optimization procedure

As mentioned above, the mesh morphing technology, the modified NSGA-II as well as the TOPSIS method are integrated into a multi-objective optimization procedure. Firstly, the mesh morphing technology is used to parameterize the sub-frame FE model for defining the design variables. The objectives and constraints of the optimization problem are also obtained through modal and strength analysis of the sub-frame. The modified NSGA-II procedure is then performed to search the Pareto solutions to the multi-objective optimization problem. After that, the TOPSIS method is adopted to determine the best compromise solution from the Pareto solutions. Fig. 5 gives a flowchart to summarize the solution procedure for this multi-objective optimization problem.

4.2 Design variables

At first, Meshworks/Morpher was used to parameterize the FE model of sub-frame using control block morphing approach due to its perfect repeatability of morphing operations. The U-shaped member and cross member have great effect on the structural strength, global stiffness and modal frequency of the sub-frame. Therefore, a total of 12 geometric parameters of the U-shaped member and cross member were defined as design variables, as described in Fig. 6. Those design variables are combination of shape changes and thickness changes. Moreover, the U-shaped member is symmetrical with respect to the longitudinal direction. The design variable x_3, x_4, x_5, x_6, x_7 and x_8 are used for determining the geometrical shape of two longitudinal beams of the U-shaped member. All design variables were considered as deviations from the initial values of the geometric parameters. The lower and upper bounds of the design variables without shape distortions are listed in Table 2.

Table 2. The range and optimization results of design variables.

Design variables	Lower bound	Baseline value	Upper bound	Point A value	Point B value
x_1	0.85	1.0	1.15	1.1181	1.0940
x_2	0.85	1.0	1.15	0.9097	0.9658
x_3	0.85	1.0	1.15	0.9127	0.8875
x_4	0.85	1.0	1.15	1.1126	1.1058
x_5	0.85	1.0	1.15	1.1369	1.1449
x_6	0.85	1.0	1.15	1.0006	0.9914
x_7	0.85	1.0	1.15	0.8916	0.8696
x_8	0.85	1.0	1.15	0.9109	0.9039
x_9 /°	-2.0	0	2.0	-0.1353	0.1081
x_{10} (mm)	-10	0	10	-5.7540	3.3577
x_{11} (mm)	1.2	2.2	3.2	2.1	2.3
x_{12} (mm)	1.5	2.5	3.5	1.8	2.1

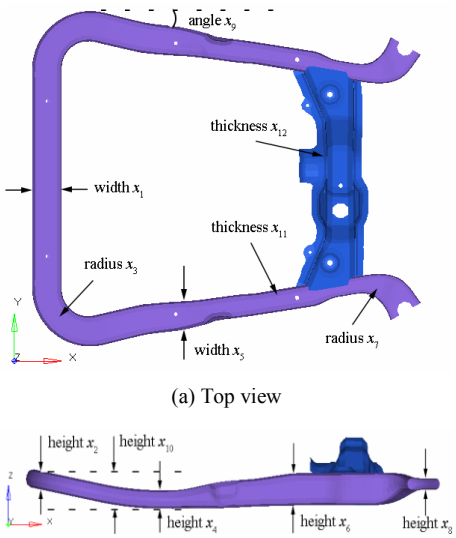

(a) Top view

(b) Lateral view

Fig. 6. Definition of design variables.

4.3 Optimization formulation

In the present study, the optimization aim is to find geomet-

rical design variables which lead to weight reduction and performance improvement of the sub-frame simultaneously. Thus, the first objective of the multi-objective optimization problem is to minimize the weight of the sub-frame. Moreover, the structural strength of the sub-frame needs to be considered in the lightweight design process. In other words, the applied stress on the sub-frame under the given load conditions should be lower than the allowable limit value, and it is also getting better as the applied stress is getting smaller. In addition, the natural frequency and stiffness of the sub-frame, which are closely related to NVH performance, should satisfy the design requirements. Therefore, the multi-objective optimization problem of the sub-frame can be formulated in the following form:

$$\begin{cases} find & \mathbf{x} = (x_1, x_2, \cdots, x_{12})^{\mathrm{T}} \\ \min & f(\mathbf{x}) = (m(\mathbf{x}), \sigma(\mathbf{x}), -f_1(\mathbf{x})) \\ s.t. & \sigma(\mathbf{x}) \le [\sigma] \\ & f_1(\mathbf{x}) \ge F_1 \\ & \Delta f_i = f_{i+1}(\mathbf{x}) - f_i(\mathbf{x}) \ge 20, i = 1, 2, \cdots, 5 \\ & d(\mathbf{x}) \le d_0 \\ & \mathbf{x}_L \le \mathbf{x} \le \mathbf{x}_U \end{cases} \tag{16}$$

where $\boldsymbol{x}$ denotes the design vector; $m(\boldsymbol{x})$ is the weight of the sub-frame; $\sigma(\boldsymbol{x})$ is the maximum von Mises stress applied to the sub-frame; $[\sigma]$ is the allowable stress set up as the yield strength of steel SAPH440, which is 305MPa; $f_i(\boldsymbol{x})$ indicates the ith order natural frequency; F_1 is the first order natural frequency of baseline design; $d(\boldsymbol{x})$ and d_0 represent the maximum values of current and initial nodal displacement, respectively, which is closely related to stiffness of the sub-frame; $\boldsymbol{x}_L$ and $\boldsymbol{x}_U$ are the lower and upper bounds of the design vector, respectively.

5. Results and discussion

5.1 Optimization results

The multi-objective optimization problem in this paper is solved by modified NSGA-II. The population size and maximum generation are set to 60 and 100, respectively. Simultaneously, a crossover probability of 0.85 and mutation probability of 0.1 are used by this algorithm. The Pareto front obtained by the modified NSGA-II is shown in Fig. 7. It consists of 306 Pareto-optimal solutions, which were obtained after 6000 evaluations.

Obviously, the Pareto front in Fig. 7 is well distributed over the entire design space, and it has satisfactory diversity characteristics. It is clear from this figure that choosing appropriate values of design variables for obtaining a better value of one objective would cause worse values of the other objectives. It indicates that these three objective functions strongly conflict with each other.

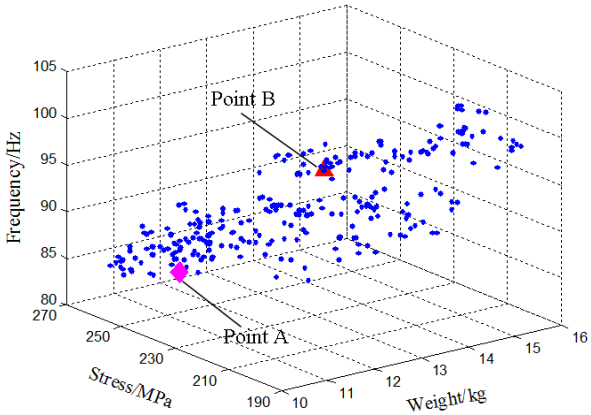

Fig. 7. Pareto front.

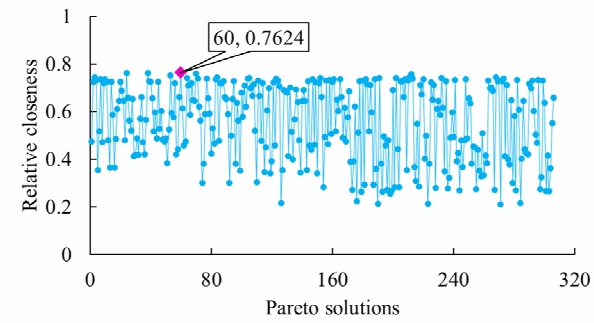

Fig. 8. The relative closeness of Pareto solutions.

5.2 TOPSIS for ranking Pareto solutions

It is now desired to find out a trade-off optimum design point from non-dominated points represented in the Pareto front compromising all objective functions. This can be achieved by TOPSIS method described in Sec. 2.3. It is obvious that the relative importance of each objective should be specified firstly for using TOPSIS method. Entropy method was used to calculate the weight of each objective. It is a vital step to obtain the final best compromise solution. The entropy weighted coefficients of the three objectives, i.e., weight, maximum von Mises stress and first order natural frequency of the sub-frame, are set as 0.5820, 0.2919 and 0.1261, respectively. Then, the relative closeness of each Pareto solution to the ideal solution is obtained, as shown in Fig. 8.

From this figure it is clear that the relative closeness reaches the maximum value of 0.7624 at the 60th Pareto solution. Therefore, this Pareto solution with the maximum value of the relative closeness is selected as the best compromise solution, which is labeled as point A in Fig. 7. Moreover, in order to investigate the superiority of the best compromise solution, another Pareto solution was selected randomly from the non-dominated points, which is marked as point B in Fig. 7. Correspondingly, the optimization results of design variables for points A and B are listed in Table 2.

Table 3. Comparison of the baseline and optimum responses.

	Baseline	Point A	Difference/%	Point B	Difference/%
m (kg)	13.27	10.95	17.46	13.16	0.84
σ (MPa)	246.10	244.57	0.62	229.05	6.93
f_1 (Hz)	86.70	85.29	1.63	95.40	-10.04
d (mm)	2.44	2.25	7.74	2.38	2.57
Δf_1 (Hz)	53.42	47.72	10.68	41.54	22.24
Δf_2 (Hz)	23.95	23.97	-0.07	21.44	10.50
Δf_3 (Hz)	57.70	59.40	-2.94	59.92	-3.85
Δf_4 (Hz)	14.17	28.34	-99.99	21.88	-54.40
Δf_5 (Hz)	37.35	21.49	42.46	25.12	32.74

5.3 Validation of the optimum design

After acquiring the best compromise solution, it is important to verify whether the result of optimization is appropriate. Thus, the resulting optimum values of the design variables are used as the input for the sub-frame FE model to perform modal and strength analysis. Table 3 shows the comparisons of simulation response values among the baseline design, points A and B.

It can be seen from this table that the weight of the sub-frame is reduced from the baseline value of 13.27 kg to 10.95 kg (i.e. a reduction of 17.46 %) at point A. Meanwhile, the maximum von Mises stress is reduced from the baseline value of 246.10 MPa to 244.57 MPa, indicating a 0.62 % reduction at point A, with a little decrease in sub-frame's the first order natural frequency (about 1.63 %). It also can be seen that all the design responses of point B have improved compared to baseline design. However, the mass reduction of the sub-frame from baseline design to point B is small (0.84 %). Therefore, the best compromise solution selected by TOPSIS method is much more preferred for the lightweight design problem.

In addition, the maximum nodal displacement of the points A and B are within the acceptable range. The intervals of neighbor order natural frequencies, which are closely related to the NVH performance, are much more reasonable than the baseline design. These results further indicate that the proposed hybrid method is feasible and effective for lightweight design of passenger car sub-frame.

6. Conclusions

In the present study, a hybrid approach is introduced for lightweight design of a passenger car sub-frame based on mesh morphing technology, modified NSGA-II and TOPSIS method. The parameterized model of the sub-frame is first developed to define the design variables based on mesh morphing technology. The multi-objective optimization problem is formulated with three conflicting objectives, including weight, maximum von Mises stress and first order natural frequency of the sub-frame. Subsequently, the modified NSGA-II, which uses ε-elimination diversity algorithm instead of crowding distance to enhance the diversity preserving performance, is used to identify the Pareto fronts. These non-dominated solutions are further analysed using TOPSIS method to rank the solutions based on their distance from the best solution and worst solution. The Shannon entropy concept is also used for computing the weights for the attributes. It is based on the information theory. The best compromise solution is then selected considering the ranking of the solutions. The results of the best compromise solution and a randomly selected Pareto solution are compared with the baseline design. According to the obtained results, it is concluded that the proposed algorithm provides well-distributed non-dominated solutions and well exploration of the research space. Moreover, the method does not impose any limitation on the number of objectives. Also, the results show that the optimal solution selected by TOPSIS method not only achieves a remarkable mass reduction compared with the baseline design, but also provides a proper compromise between weight and structural performance of the sub-frame compared with other Pareto points. The proposed hybrid method is proved to be feasible and effective for lightweight design of passenger car sub-frame.

Acknowledgment

This research work was supported by National New Energy Vehicle Pilot Project (2016YFB0101601), Chongqing Basis and Leading-edge Research Program Projects (cstc2013 jcyjC60001) and Graduate Innovation Fund of Jilin University (No. 2015084). The authors would like to express their appreciations for the above fund supports.

Nomenclature

$\boldsymbol{D}_i$: Displacement vector
$\boldsymbol{TM}$: Transformation matrix
$\boldsymbol{CN}_i$: The vector of control node coordinates
α : Rotation around local Z-axis
β : Rotation around local Y-axis
γ : Rotation around local X-axis
$\boldsymbol{DN}_i^{current}$: Current position of deformable node
$\boldsymbol{DN}_i^{new}$: New position of deformable node
CD_i^k : Crowding distance
CD^k : Overall crowding distance
$\boldsymbol{X}$: Decision making matrix
x_{ij} : Result of jth objective function for ith Pareto solution
r_{ij} : Normalized value of x_{ij}
e_j : Entropy value
p_{ij} : Projection value of r_{ij}
w_j : Weight value of jth objective
v_{ij} : Weighted normalized value of x_{ij}
A^+ : Positive ideal solution
A^- : Negative ideal solution

S_i^+ : Distance between the ith alternative and PIS
S_i^- : Distance between the ith alternative and NIS
C_i : Relative closeness of alternative i
$f(\boldsymbol{x})$: Objective function
$m(\boldsymbol{x})$: Weight of sub-frame
$\sigma(\boldsymbol{x})$: Maximum von Mises stress applied on sub-frame
$f_i(\boldsymbol{x})$: The ith order natural frequency
$[\sigma]$: Allowable stress
Δf_i : Interval between neighbor order frequencies
F_1 : First order natural frequency of baseline design
$d(\boldsymbol{x})$: Maximum value of nodal displacement
d_0 : Initial value of maximum nodal displacement
$\boldsymbol{x}_L$: Lower bound of design vector
$\boldsymbol{x}_U$: Upper bound of design vector

References

[1] G. Belingardi and E. G. Koricho, Design of a composite engine support sub-frame to achieve lightweight vehicles, *International Journal of Automotive Composites*, 1 (1) 2014 90-111.

[2] P. Zhu, Y. Zhang and G. L. Chen, Metamodel-based lightweight design of an automotive front-body structure using robust optimization, *Proceedings of the Institution of Mechanical Engineers, Part D: Journal of Automobile Engineering*, 223 (9) (2009) 1133-1147.

[3] F. Pan, P. Zhu and Y. Zhang, Metamodel-based lightweight design of B-pillar with TWB structure via support vector regression, *Computers & Structures*, 88 (1) (2010) 36-44.

[4] M. N. Velea, P. Wennhage and D. Zenkert, Multi-objective optimisation of vehicle bodies made of FRP sandwich structures, *Composite Structures*, 111 (2014) 75-84.

[5] H. Ye, P. Hu and G. Z. Shen, Lightweight optimization design of car body based on sensitivity and side crash simulation, *Transactions of the Chinese Society for Agricultural Machinery*, 41 (10) (2010) 18-22.

[6] R. Padmanaban et al., Multi-disciplinary optimization of a sport utility vehicle, *SAE Paper*, 2004-05AE-271 (2004).

[7] Y. Wang et al., A research on the application of mesh morphing technology to car body retrofit design, *Automotive Engineering*, 9 (2012) 847-851.

[8] J. G. Fang et al., Multi-objective shape optimization of body-in-white based on mesh morphing technology, *Journal of Mechanical Engineering*, 48 (24) (2013) 119-126.

[9] P. Wang and G. Wu, Multidisciplinary design optimization of vehicle instrument panel based on multi-objective genetic algorithm, *Chinese Journal of Mechanical Engineering*, 26 (2) (2013) 304-312.

[10] K. Deb et al., A fast and elitist multiobjective genetic algorithm: NSGA-II, *IEEE Transactions on Evolutionary Computation*, 6 (2) (2002) 182-197.

[11] X. Cui, S. Wang and S. J. Hu, A method for optimal design of automotive body assembly using multi-material construction, *Materials & Design*, 29 (2) (2008) 381-387.

[12] R. Y. Su, L. J. Gui and Z. J. Fan, Multi-objective optimization for bus body with strength and rollover safety constraints based on surrogate models, *Structural and Multidisciplinary Optimization*, 44 (3) (2011) 431-441.

[13] Z. Hu, A. Cheng and S. Chen, Applications of multi-objective optimization to new vehicle overall lightweight design, *China Mechanical Engineering*, 24 (3) (2013) 404-409.

[14] N. Nariman-Zadeh et al., Pareto optimization of a five-degree of freedom vehicle vibration model using a multi-objective uniform-diversity genetic algorithm (MUGA), *Engineering Applications of Artificial Intelligence*, 23 (4) (2010) 543-551.

[15] H. Van der Auweraer et al., Application of mesh morphing technology in the concept phase of vehicle development, *International Journal of Vehicle Design*, 43 (1-4) (2007) 281-305.

[16] K. P. Yoon and C. L. Hwang, *Multiple attribute decision making: an introduction*, Sage Publication, Thousands Oaks, CA (1995).

[17] R. Adalarasan and A. Shanmuga Sundaram, Parameter design and analysis in continuous drive friction welding of Al6061/SiCp composites, *Journal of Mechanical Science and Technology*, 29 (2) (2015) 769-776.

[18] T.-P. Dao and S.-C. Huang, Robust design for a flexible bearing with 1-DOF translation using the Taguchi method and the utility concept, *Journal of Mechanical Science and Technology*, 29 (8) (2015) 3309-3320.

[19] R. Manivannan and M. P. Kumar, Multi-response optimization of Micro-EDM process parameters on AISI304 steel using TOPSIS, *Journal of Mechanical Science and Technology*, 30 (1) (2016) 137-144.

Dengfeng Wang is a Professor of Vehicle Engineering at College of Automotive Engineering, Jilin University, China. He received his B.Sc., M.Sc. and Ph.D. from the Jilin University of Technology in 1984, 1987 and 1990, respectively. He was a Senior Visiting Scholar in the University of Birmingham from 1997 to 1998. His research interests include vehicle dynamics and control, numerical optimization, vehicle NVH analysis and control, and vehicle lightweight design.

Rongchao Jiang received his Ph.D. degree in Vehicle Engineering from Jilin University, China, in 2016. He is currently a Lecturer of Vehicle Engineering at Qingdao University, China. His research interests are vehicle dynamics and control, optimization techniques, and vehicle lightweight design.